

Certified Approximation Algorithms for the Fermat Point and n -Ellipses

Kolja Junginger ✉

Faculty of Informatics, Università della Svizzera italiana, Lugano, Switzerland

Ioannis Mantas ✉ 

Faculty of Informatics, Università della Svizzera italiana, Lugano, Switzerland

Evanthia Papadopoulou ✉ 

Faculty of Informatics, Università della Svizzera italiana, Lugano, Switzerland

Martin Suderland ✉ 

Faculty of Informatics, Università della Svizzera italiana, Lugano, Switzerland

Chee Yap ✉ 

Courant Institute, NYU, New York, NY, USA

Abstract

Given a set A of n points in \mathbb{R}^d with weight function $w : A \rightarrow \mathbb{R}_{>0}$, the Fermat distance function is $\varphi(\mathbf{x}) = \sum_{\mathbf{a} \in A} w(\mathbf{a}) \|\mathbf{x} - \mathbf{a}\|$. A classic problem in facility location dating back to 1643, is to find the *Fermat point* \mathbf{x}^* , the point that minimizes the function φ . In general, the Fermat point \mathbf{x}^* cannot be computed exactly, so finding fast approximation algorithms has been of particular interest. In this work, we present algorithms to compute an ε -approximation of the Fermat point \mathbf{x}^* , that is, a point $\tilde{\mathbf{x}}^*$ satisfying $\|\tilde{\mathbf{x}}^* - \mathbf{x}^*\| < \varepsilon$. Our approximation scheme differs from the usual $\varphi(\tilde{\mathbf{x}}^*) \leq (1 + \varepsilon)\varphi(\mathbf{x}^*)$ approximation considered in the literature, which approximates the distance function. Our ε -approximation of the Fermat point directly implies an ε -approximation of the distance function, whereas the converse is not possible.

Our algorithms are based on the *subdivision* paradigm, which we enhance with Newton methods, used for *certification*, in the sense of *interval methods*, and for speed-ups. Moreover, we consider the problem of constructing *n-ellipses*, which are the r -level sets $\varphi^{-1}(r)$. The notion of an n -ellipse is a generalization of the classic (2-)ellipse and the circle (1-ellipse). Using the subdivision paradigm, we design an ε -isotopic approximation algorithm to compute n -ellipses in \mathbb{R}^2 . We have implemented our algorithms and we provide an experimental analysis using different point configurations and heuristics for speed-ups. The obtained results suggest the practicality of our approaches especially in low dimensions and for small epsilon.

2012 ACM Subject Classification Theory of computation \rightarrow Approximation algorithms analysis

Keywords and phrases Fermat point, n -ellipse, subdivision, approximation, certified, algorithms

Digital Object Identifier 10.4230/LIPIcs.ESA.2021.49

Related Version arXiv

Funding The work of C. Yap was supported by an USI Visiting Professor Fellowship (Fall 2018); additional support came from NSF Grants # CCF-1564132 and # CCF-2008768. Other authors were partially supported by SNF 200021E_154387.



© Kolja Junginger, Ioannis Mantas, Evanthia Papadopoulou, Martin Suderland, and Chee Yap; licensed under Creative Commons License CC-BY 4.0

29th Annual European Symposium on Algorithms (ESA 2021).

Editors: Petra Mutzel, Rasmus Pagh, and Grzegorz Herman; Article No. 49; pp. 49:1–49:19

Leibniz International Proceedings in Informatics



LIPICs Schloss Dagstuhl – Leibniz-Zentrum für Informatik, Dagstuhl Publishing, Germany

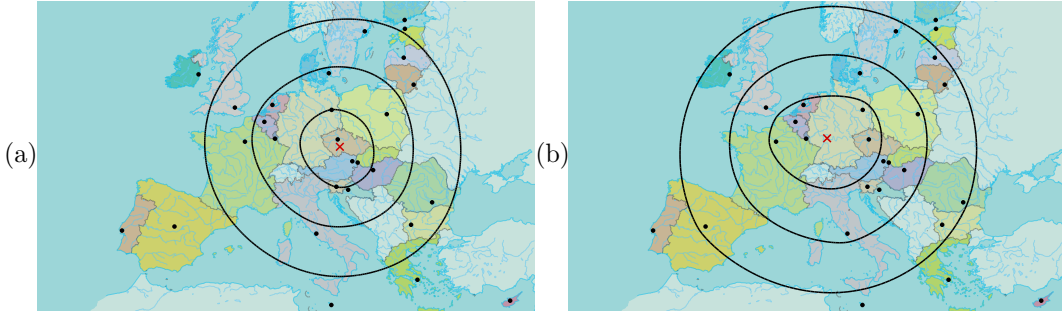


Figure 1 The Fermat point of the 28 EU-capitals (pre-Brexit), highlighted with (x), along with three 28-ellipses of different radii. (a) The foci (capitals) are unweighted. (b) Each foci has the weight of the country’s population. The source of the map is <https://www.consilium.europa.eu>.

38 **1 Introduction**

39 A classic problem in Facility Location, see e.g., [21, 43], is the placement of a facility to
 40 serve a given set of demand points or customers so that the total transportation costs are
 41 minimized. The total cost at any point is interpreted as the sum of the distances to the
 42 demand points. The point that minimizes this sum is called the *Fermat Point*; see Fig. 1.
 43 This is an old geometric problem that has inspired scientists over the last three centuries.

44 A *weighted foci set* is a non-empty finite set of (demand) points $A = \{\mathbf{a}_1, \dots, \mathbf{a}_n\}$ in \mathbb{R}^d
 45 associated with a positive weight function $w : A \rightarrow \mathbb{R}_{>0}$. Each $\mathbf{a} \in A$ is called a *focus* with
 46 weight $w(\mathbf{a})$. Let $W = \sum_{\mathbf{a} \in A} w(\mathbf{a})$. The *Fermat distance function* of A is given by

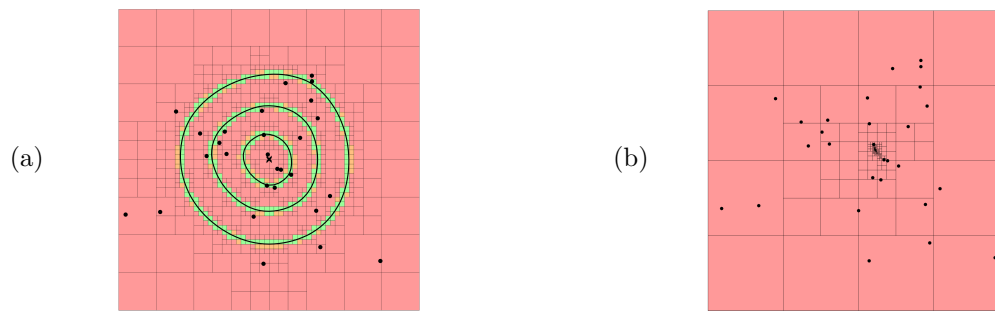
$$\varphi(\mathbf{x}) := \sum_{\mathbf{a} \in A} w(\mathbf{a}) \|\mathbf{x} - \mathbf{a}\|,$$

47 where $\|\cdot\|$ is the Euclidean norm in \mathbb{R}^d . The global minimum value of φ is called the *Fermat*
 48 *radius* of A and denoted r^* ; any point $\mathbf{x} \in \mathbb{R}^d$ that achieves this minimum, $\varphi(\mathbf{x}) = r^*$, is
 49 called a *Fermat point* and denoted $\mathbf{x}^* = \mathbf{x}^*(A)$. The Fermat point is not unique if and only
 50 if A is collinear and n is even. We can check if A is collinear in $O(n)$ time, and in that case,
 51 the median, which is a Fermat point, can be found in $O(n \log n)$ time. So henceforth, we
 52 assume that A is not collinear, thus φ is a strictly convex function [35, 37], and \mathbf{x}^* is unique.

53 We also consider the closely related problem of computing *n-ellipses* of A . For any
 54 $r > r^*(A)$, the level set of the Fermat distance function is $\varphi^{-1}(r) := \{\mathbf{x} \in \mathbb{R}^d : \varphi(\mathbf{x}) = r\}$.
 55 If $n = 1$, the level set is a sphere; and if $n = 2$ and $d = 2$, it is the classic ellipse. When
 56 A has n points, we call $\varphi^{-1}(r)$ an *n-ellipsoid*, or an *n-ellipse* if $d = 2$; hence the term *foci*
 57 *set*. From an application perspective, an *n-ellipse* of radius r can be viewed as a curve that
 58 bounds the candidate area for facility location [46], such that the total transportation cost
 59 to the demand points is at most some specified r , as in Fig. 1.

60 The question of approximating the Fermat point is of great interest as its coordinates
 61 are the solution of a polynomial with exponentially high degree [3], thus when $n > 4$ the
 62 exact solution cannot be found in the general case. We address the problem of computing
 63 an ε -approximation $\tilde{\mathbf{x}}^*$ to the Fermat point \mathbf{x}^* , where ε is an arbitrarily small positive real
 64 number. This can be interpreted in 3 ways:

- 65 (A) **Approximate Fermat Point:** $\|\tilde{\mathbf{x}}^* - \mathbf{x}^*\| \leq \varepsilon$;
- 66 (B) **Absolute Approximate Fermat Radius:** $\varphi(\tilde{\mathbf{x}}^*) \leq \varphi(\mathbf{x}^*) + \varepsilon$;
- 67 (C) **Relative Approximate Fermat Radius:** $\varphi(\tilde{\mathbf{x}}^*) \leq (1 + \varepsilon)\varphi(\mathbf{x}^*)$.



■ **Figure 2** The resulting box subdivision of Fig. 1(a) for (a) the n -ellipses and (b) the Fermat point.

68 We show that senses (B) and (C) can be reduced to (A), whereas the converse is not clear.
 69 Essentially (B) and (C) are approximations of the Fermat radius, and sense (A) is stronger.
 70 In this paper we consider approximations in the sense (A); to the best of our knowledge, only
 71 approximations (B) and (C), have been considered before, see e.g., [8, 16],

72 In this work we introduce certified algorithms for approximating the Fermat point and n -
 73 ellipses, combining a subdivision approach with interval methods (cf. [33, 48]). The approach
 74 can be formalized in the framework of “soft predicates” [56]. Our certified algorithms are
 75 fairly easy to implement, and are shown to have good performance experimentally.

76 **Related Work.** The problem we study has a long history, with numerous extensions and
 77 variations. Out of the 15 names found in the literature, see [23], we call it *the Fermat point*
 78 *problem*. Other common names are the *Fermat-Weber problem* and the *Geometric median*
 79 *problem*. Apart from the Facility Location application introduced by Weber [57], the problem
 80 is motivated by applications in diverse fields such as statistics and data mining where it is
 81 known as the *1-Median problem*, and is an instance of the k -median clustering technique [27].

82 For $d = 2, n = 3$, the problem was first stated by P. Fermat (1607 - 1665) and was solved
 83 by E. Torricelli (1608 - 1647) and Krarup and Vajda [30] using a geometric construction.
 84 For $n = 4$, solutions were given by Fagnano [20] and Cieslik [14]. The first general method,
 85 for arbitrary n , is an iterative scheme proposed by Weiszfeld [58] in 1937. It was later
 86 corrected and improved by Kuhn [32] and Ostresh [43]; see Beck and Sabach [4] for a review.
 87 The method which is essentially a gradient descent, implies an iterative algorithm with no
 88 asymptotic runtime complexity, which can behave quite well in practice.

89 A plethora of approximation algorithms for the Fermat point, in senses (B) and (C), can
 90 be found in the literature using various methods. There are algorithms based on semidefinite
 91 programming [45], interior point methods [16, 60], sampling [2, 16], geometric data structures
 92 [8] and coresets [26], among others [13, 22]. Moreover, special configurations of foci have
 93 been considered [7, 15], a continuous version of the problem [21], and the problem of finding
 94 the Fermat point of planar convex objects [1, 12, 18].

95 The literature on n -ellipses is smaller but equally old: Nagy [38] proved that n -ellipses are
 96 convex curves, calling them *egg curves*, and dating them back to Tschirnhaus in 1695 [55,
 97 p. 183]. Further, he characterized the singular points of the n -ellipses as being either foci or
 98 the Fermat point. Another early work is by Sturm in 1884 [53]. Sekino [51] showed that the
 99 Fermat distance function φ is C^∞ on $\mathbb{R}^2 \setminus A$. So, the n -ellipse is a piecewise smooth curve,
 100 as it may pass through several foci. Nie et al. [42] showed that the polynomial equation
 101 defining the n -ellipses has algebraic degree exponential in n .

102 **Our Contributions.** In this paper, we design, implement and experimentally evaluate
 103 algorithms for approximating the Fermat point of a given set of foci in \mathbb{R}^d . We also compute
 104 an ε -approximate n -ellipse; a problem not considered in computational literature before.
 105 These are the first certified algorithms [36, 54] for these problems. Our contributions are
 106 summarized as follows:

- 107 ■ We design two certified algorithm for approximate Fermat point: one is based on subdivi-
 108 sion, the other based on Weiszfeld iteration [58].
- 109 ■ Our notion of ε -approximate Fermat point appears to be new; in contrast, several recent
 110 works focus on ε -approximation of the Fermat radius. The approximate Fermat radius
 111 can be reduced to approximate Fermat point; the converse reduction is unclear.
- 112 ■ Based on the *PV construction* [47, 33], we design an algorithm to compute a regular
 113 isotopic ε -approximation of an n -ellipse. We also augment the algorithm to compute
 114 simultaneous contour plots of the distance function φ , resulting in a useful visualization
 115 tool (see Fig. 1).
- 116 ■ We implement our algorithms and experiment with different datasets and speedups. Each
 117 method is evaluated based on different values of the input parameters.

118 Various details of the interval primitives and proofs can be found in the full arXiv version.

119 2 Preliminaries

120 Vector variables are written in bold font: thus $\mathbf{0}$ is the origin of \mathbb{R}^d and $\mathbf{x} = (x_1, \dots, x_n)$.
 121 Let $\partial_i f$ denote partial differentiation with respect to x_i . The *gradient* $\nabla f : \mathbb{R}^d \rightarrow \mathbb{R}^d$ of f is
 122 given by the vector $\nabla f(\mathbf{x}) = (f_1(\mathbf{x}), \dots, f_n(\mathbf{x}))^T$ where $f_i = \partial_i f$. In general, the operator
 123 ∇ is partial, i.e., $\nabla f(\mathbf{x}_0)$ might not be defined at a point \mathbf{x}_0 . A point \mathbf{x}_0 is a *critical point*
 124 of f if $\nabla f(\mathbf{x}) = \mathbf{0}$ or $\nabla f(\mathbf{x})$ is undefined.

125 We consider analytic properties of a scalar function $f : \mathbb{R}^d \rightarrow \mathbb{R}$, mainly from the viewpoint
 126 of convex analysis [35, 39]. In our case, f is the Fermat distance function for some weighted
 127 set A . From a general perspective the Fermat point problem (resp., n -ellipsoid problem)
 128 reduces to computing the critical points of the gradient of f (resp., computing the level sets
 129 of f). The Fermat point is the only critical point of f in $\mathbb{R}^d \setminus A$ assuming A is non-collinear.

130 Most of the basic properties regarding the Fermat point are well-known and may be found
 131 in our references such as [32, 35, 39, 43, 58]. To emphasize the foci set A , we explicitly write
 132 φ_A instead of φ . A focus $\mathbf{a} \in A$ is the Fermat point of A if and only if $\|\nabla \varphi_{A \setminus \mathbf{a}}(\mathbf{a})\| \leq w(\mathbf{a})$.
 133 Testing if the Fermat point \mathbf{x}^* is in A can be done in $O(n^2d)$ time. If \mathbf{x}^* is not one of the
 134 foci, then $\nabla f(\mathbf{x}^*) = \mathbf{0}$, and the problem can be reduced to general finding zeros of a system
 135 of equations (e.g., [59]). The thrust of this paper is to develop direct methods that exploit
 136 the special properties of the Fermat problem.

137 We formally define the two main problems which we consider:

- 138 ■ APPROXIMATE FERMAT POINT: Given a weighted point set A in \mathbb{R}^d and $\varepsilon > 0$, compute
 139 a point $\tilde{\mathbf{x}}^*$ within ε distance to the Fermat point \mathbf{x}^* of A .
- 140 ■ APPROXIMATE ISOTOPIC n -ELLIPSES: Given $\varepsilon > 0$, a weighted point set A in \mathbb{R}^2 of
 141 size n and a radius $r > r^*(A)$, compute a closed polygonal curve E that is ε -isotopic to
 142 $\varphi^{-1}(r)$, i.e., there exists an ambient isotopy¹ $\gamma : \mathbb{R}^2 \times [0, 1] \rightarrow \mathbb{R}^2$ with $\gamma(E, 1) = \varphi^{-1}(r)$
 143 and for any point $\mathbf{a} \in \varphi^{-1}(r)$, the parametric curve $\gamma(\mathbf{a}, \cdot)$ has at most length ε . This
 144 implies a bound of ε on the Hausdorff distance between E and $\varphi^{-1}(r)$.

¹ That is, a continuous map $\gamma : \mathbb{R}^2 \times [0, 1] \rightarrow \mathbb{R}^2$ such that $\gamma_0 = \gamma(\cdot, 0)$ is the identity map, and, for all $t \in [0, 1]$, $\gamma_t = \gamma(\cdot, t)$ is a homeomorphism on \mathbb{R}^2 .

Approximation notions. We compare the three different notions of ε -approximation for the Fermat point. We reduce the approximation problem of notion (C) to (B), and (B) to (A). An ε -approximation $\tilde{\mathbf{x}}^*$ of \mathbf{x}^* in the sense $\|\tilde{\mathbf{x}}^* - \mathbf{x}^*\| \leq \varepsilon$ is also a $(W\varepsilon)$ -approximation in the sense $\varphi(\tilde{\mathbf{x}}^*) \leq \varphi(\mathbf{x}^*) + W\varepsilon$, which follows directly from the triangle inequality

$$\varphi(\tilde{\mathbf{x}}^*) = \sum_{\mathbf{a} \in A} w(\mathbf{a}) \|\tilde{\mathbf{x}}^* - \mathbf{a}\| \leq \sum_{\mathbf{a} \in A} w(\mathbf{a}) (\|\tilde{\mathbf{x}}^* - \mathbf{x}^*\| + \|\mathbf{x}^* - \mathbf{a}\|) = W\varepsilon + \varphi(\mathbf{x}^*).$$

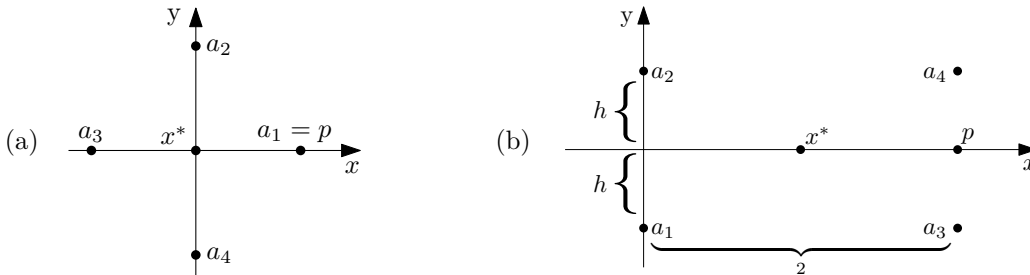
An ε -approximation $\tilde{\mathbf{x}}^*$ of \mathbf{x}^* in the sense $\varphi(\tilde{\mathbf{x}}^*) \leq \varphi(\mathbf{x}^*) + \varepsilon$ is also a $\frac{2\varepsilon}{\varphi(g)}$ -approximation in the sense $\varphi(\tilde{\mathbf{x}}^*) \leq (1 + \frac{2\varepsilon}{\varphi(g)})\varphi(\mathbf{x}^*)$. The center of gravity g is a 2-approximation of the Fermat radius r^* (see [16]), i.e. $\varphi(\mathbf{x}^*) \geq \frac{1}{2}\varphi(g)$. Hence

$$\varphi(\tilde{\mathbf{x}}^*) \leq \varphi(\mathbf{x}^*) + \varepsilon = \left(1 + \frac{\varepsilon}{\varphi(\mathbf{x}^*)}\right) \varphi(\mathbf{x}^*) \leq \left(1 + \frac{2\varepsilon}{\varphi(g)}\right) \varphi(\mathbf{x}^*)$$

145 On the other hand, it is not clear how to derive an ε -approximation of type (A) if an
 146 approximation algorithm for type (B) and (C) is at hand, as the following 2 examples show.

147 **Example 1:** For any $\varepsilon > 0$ choose $c \leq \frac{\varepsilon}{2\sqrt{2}-2}$ and consider the weighted foci $\mathbf{a}_1 = (1, 0)$,
 148 $\mathbf{a}_2 = (0, 1)$, $\mathbf{a}_3 = (-1, 0)$, $\mathbf{a}_4 = (0, -1)$ with $w(\mathbf{a}_1) = w(\mathbf{a}_3) = 1$ and $w(\mathbf{a}_2) = w(\mathbf{a}_4) = c$ for
 149 which the Fermat point is $\mathbf{x}^* = (0, 0)$ for symmetry reasons, see Fig. 3(a). Point $p = (1, 0)$ is
 150 an ε -approximation of \mathbf{x}^* in the sense (B) and (C), but it has a distance of 1 to \mathbf{x}^* .

151 **Example 2:** For any $\varepsilon > 0$ we choose $h > 0$ small enough such that: $2\sqrt{4+h^2} + 2h \leq$
 152 $4\sqrt{1+h^2} + \varepsilon$. Consider the foci $\mathbf{a}_1 = (0, -h)$, $\mathbf{a}_2 = (0, h)$, $\mathbf{a}_3 = (2, -h)$, $\mathbf{a}_4 = (2, h)$ with unit
 153 weights. The Fermat point is $\mathbf{x}^* = (1, 0)$ for symmetry reasons, see Fig. 3(b). Point $p = (2, 0)$
 154 is an ε -approximation of \mathbf{x}^* in the sense (B) and (C), but it has a distance of 1 to \mathbf{x}^* .



■ **Figure 3** Examples that a *good* approximation of the Fermat point (a) in sense (B) or (b) in sense (C), does not imply a *good* approximation in sense (A).

155 **Subdivision Paradigm.** The subdivision algorithms presented in this paper take as input an
 156 initial box $B_0 \subset \mathbb{R}^d$ and recursively split it. We organize the boxes in a *generalized quadtree*
 157 data structure [50]. A box can be specified by d intervals as $B = I_1 \times I_2 \times \dots \times I_d$. Let
 158 m_B denote the *center* of B , r_B the *radius* of B (distance between m_B and a corner), and
 159 $\omega(B)$ the *width* of B (the maximum length of its defining intervals). The term $c \cdot B$ denotes
 160 the box with center m_B and radius $c \cdot r_B$. The function SPLIT_1 takes a box B and returns
 161 2^d congruent subboxes (*children*), one for each orthant. We use SPLIT_2 to indicate that we
 162 do two successive levels of SPLIT_1 operations (i.e., $1 + 2^d$ SPLIT_1 operations, resulting in
 163 $(2^d)^2 = 4^d$ leaves).

164 **Soft Predicates.** Let $\square \mathbb{R}^d$ denote the set of closed d -dimensional boxes (i.e., Cartesian
 165 products of intervals) in \mathbb{R}^d . Let P be a logical *predicate* on boxes, i.e., $P : \square \mathbb{R}^d \rightarrow$

166 $\{\mathbf{true}, \mathbf{false}\}$. For example, the Fermat point predicate is given by $P_{\text{FP}}(B) = \mathbf{true}$ if and
 167 only if $\mathbf{x}^* \in B$. Logical predicates are hard to implement, and thus, we may focus on
 168 *tests*, which are viewed as “one-sided predicates”. Formally, a test T looks like a predicate:
 169 $T : \square \mathbb{R}^d \rightarrow \{\mathbf{success}, \mathbf{failure}\}$ and it is always associated to some predicate P : call T a
 170 *test for predicate P* if $T(B) = \mathbf{success}$ implies $P(B) = \mathbf{true}$. However, we conclude nothing
 171 if $T(B) = \mathbf{failure}$. Denote this relation by “ $T \Rightarrow P$ ”.

172 Soft predicates [56] are an intermediate concept between a test and a predicate. Typically,
 173 they arise from a partial scalar function $f : \mathbb{R}^d \rightarrow \mathbb{R} \cup \{\uparrow\}$ where $f(\mathbf{x}) = \uparrow$ means $f(\mathbf{x})$ is not
 174 defined. We then define a partial *geometric predicate* P_f on boxes B as follows:

$$P_f(B) = \begin{cases} \uparrow & \text{if } \uparrow \in f(B), \\ +1 & \text{if } f(B) > 0, \\ -1 & \text{if } f(B) < 0, \\ 0 & \text{else.} \end{cases}$$

175 We can now derive various logical predicates P from P_f , by identifying the values in
 176 the set $\{-1, 0, +1, \uparrow\}$ with \mathbf{true} or \mathbf{false} . For instance, we call P an *exclusion predicate*
 177 if we associate the 0- and \uparrow -value with \mathbf{false} and the other values with \mathbf{true} . For the
 178 *inclusion* predicate, we associate the 0-value with \mathbf{true} , others with \mathbf{false} . For example,
 179 a test for the Fermat point predicate P_{FP} is an inclusion predicate based on the partial
 180 function $f(\mathbf{x}) = \sum_i (\partial_i f(\mathbf{x}))^2$; the function is partial because $f(\mathbf{x}) = \uparrow$ when \mathbf{x} is a focus
 181 point. Although our box predicates $P(B)$ are defined for full-dimensional boxes B , we
 182 can extend them to any point \mathbf{x} as follows: $P(\mathbf{x})$ has the logical value associated with the
 183 $\text{sign}(f(\mathbf{x})) \in \{\uparrow, +1, -1, 0\}$.

184 **► Definition 1.** Let T be a test for a predicate P . We call T a *soft predicate* (or *soft version*
 185 *of P*) if it is convergent in this sense: if $(B_i : i = 0, 1, \dots)$ is a monotone sequence of boxes
 186 $B_{i+1} \subseteq B_i$ that converges to a point \mathbf{a} , then $P(\mathbf{a}) \equiv T(B_i)$ for i large enough.

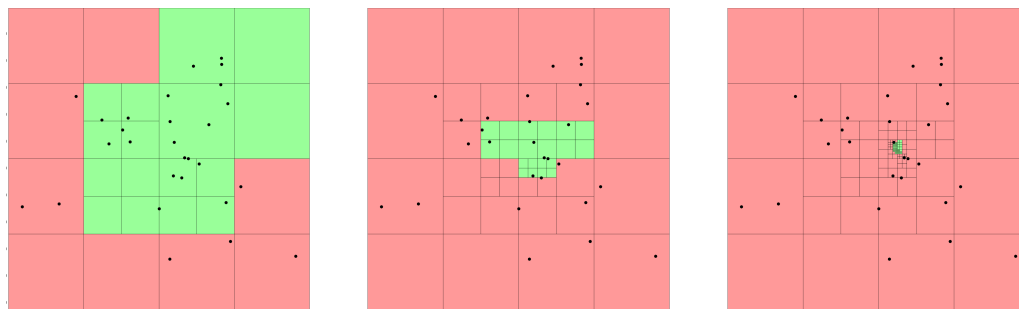
187 Here, “ $P(\mathbf{a}) \equiv T(B_i)$ ” means $P(\mathbf{a}) = \mathbf{true}$ iff $T(B_i) = \mathbf{success}$. A soft version of $P(B)$
 188 is usually denoted $\square P(B)$. We note that soft versions of exclusion predicates are generally
 189 easier to construct than inclusion predicates. The former can be achieved by numerical
 190 approximation, while the latter requires some deeper principle such as the Brouwer fixed
 191 point theorem [9].

192 **Interval arithmetic.** We construct soft predicates using functions of the form $F : \square \mathbb{R}^d \rightarrow$
 193 $\square(\mathbb{R} \cup \{-\infty, \infty\})$ that approximates the scalar function $f : D \rightarrow \mathbb{R}$ with $D \subset \mathbb{R}^d$.

194 **► Definition 2.** Call F a *soft version of f* if it is
 195 *i)* conservative, i.e. for all $B \in \square \mathbb{R}^d$, $F(B)$ contains $f(B) := \{f(p) : p \in B \cap D\}$, and
 196 *ii)* convergent, i.e. if for monotone sequence $(B_i : i \geq 0)$ that converges to a point $\mathbf{a} \in D$,
 197 $\lim_{i \rightarrow \infty} \omega(F(B_i)) = 0$ holds.

198 We shall denote F by $\square f$ when F is a soft version of f . There are many ways to
 199 achieve $\square f$. E.g., f has an arithmetic expression E , we can simply evaluate E using interval
 200 arithmetic. More sophisticated methods may be needed for performance. The next lemma
 201 shows how $\square f$ leads to soft exclusion predicates based on f :

202 **► Lemma 3.** If P is an exclusion predicate based on f , then the test $\square P(B) : 0 \notin \square f(B)$ is
 203 a *soft version of P* .



■ **Figure 4** Different steps during the the execution of Algorithm 1. The dark red boxes cannot contain the Fermat point, whereas the light green boxes may contain it.

204 Below, we need a multivariate generalization, to the case where $\mathbf{f} : \mathbb{R}^d \rightarrow \mathbb{R}^m$, and the
 205 exclusion predicate $P(B)$ is $\mathbf{0} \notin \mathbf{f}(B)$. If $\square\mathbf{f} : \square\mathbb{R}^d \rightarrow \square\mathbb{R}^m$ is a soft version of \mathbf{f} , then a
 206 soft version of $P(B)$ is the given by the test $T(B) : \mathbf{0} \notin \square\mathbf{f}(B)$. If $\mathbf{f} = (f_1, \dots, f_m)$, then
 207 this reduces to $0 \notin \square f_i(B)$ for some $i = 1, \dots, m$.

208 3 Approximate Fermat points

209 We now present three approximation algorithms for the Fermat point \mathbf{x}^* . For simplicity, we
 210 assume in our algorithms that the Fermat point is not a focus, i.e. $\mathbf{x}^* \notin A$. This assumption
 211 can be easily checked in $O(n^2d)$ preprocessing time, or with a more elegant approach, in
 212 $O(nd)$ time during the execution of our subdivision algorithms.

213 3.1 Using the Subdivision Paradigm

214 The subdivision paradigm requires an initial box B_0 to start subdividing. If B_0 is not given,
 215 it is easy to find a box that contains \mathbf{x}^* , since \mathbf{x}^* lies in the convex hull of A [32]. We use
 216 a function INITIAL-BOX(A) which, in $O(nd)$ time, computes an axis-aligned bounding box
 217 with corners having the minimum and maximum x, y coordinates.

218 We define an exclusion and inclusion predicate based on the gradient function $\nabla\varphi$.

219 ► **Definition 4.** Given a box B , the gradient exclusion predicate $C_0^\nabla(B)$ is defined by the
 220 condition $\mathbf{0} \notin \nabla\varphi(B)$. The gradient inclusion predicate $C_1^\nabla(B)$ is just the complement of
 221 $C_0^\nabla(B)$, $\mathbf{0} \in \nabla\varphi(B)$.

222 Under our assumptions that $\mathbf{x}^* \notin A$, we have $C_1^\nabla(B)$ holds iff $\mathbf{x}^* \in B$. We obtain a soft
 223 version of the exclusion predicate $C_0^\nabla(B)$ by replacing $\nabla\varphi$ in its definition with any soft
 224 version $\square\nabla\varphi$, see Lemma 3. But it is not so easy to get a soft version of $C_1^\nabla(B)$; we shall
 225 return to this when we treat the Newton operator below.

226 In Algorithm 1, using the exclusion predicate we discard boxes that are guaranteed not
 227 to contain \mathbf{x}^* (red in Fig. 4) and we split boxes that might contain \mathbf{x}^* (green in Fig. 4).
 228 While subdividing, we test whether we can already approximate \mathbf{x}^* well enough by putting a
 229 bounding box around all the (green) boxes that are not excluded yet, using the following
 230 predicate.

231 ► **Definition 5.** Given a set of boxes Q that contains the Fermat point, the stopping predicate
 232 $C^\varepsilon(Q)$ returns true, if and only if the minimum axis-aligned bounding box containing all
 233 boxes in Q has a radius at most ε .

234 If C^ε returns true, then we can stop. Since the radius of the minimum bounding box is
 235 at most ε , the center of the box is an ε -approximate Fermat point $\tilde{\mathbf{x}}^*$.

■ **Algorithm 1** Subdivision for the approximate Fermat point (*SUB*)

Input : Foci set A , constant $\varepsilon > 0$
Output: Point $\tilde{\mathbf{x}}^*$

```

1  $B_0 \leftarrow \text{INITIAL-BOX}(A)$ ;  $Q \leftarrow \text{QUEUE}()$ ;  $Q.\text{PUSH}(B_0)$ ;
2 while not  $C^\varepsilon(Q)$  do
3    $B \leftarrow Q.\text{POP}()$ ;
4   if not  $\square C_0^\nabla(B)$  then
5      $Q.\text{PUSH}(\text{SPLIT}_1(B))$ ;
6 return  $\tilde{\mathbf{x}}^* \leftarrow \text{Center of the bounding box of } Q$ ;
```

236 Regarding the runtime of Algorithm 1, evaluating $\nabla\varphi$ and its soft version takes linear
 237 time in n . The subdivision approach induces an exponential dependency on d , as splitting
 238 a box creates 2^d many children. Further, a SPLIT_1 operation decreases the boxwidth by a
 239 factor of 2, therefore, Algorithm 1 cannot converge faster than linear in ε .

240 3.2 Enhancing the Subdivision Paradigm

241 In this section, we augment Algorithm 1 with a speed up based on a *Newton operator*, which
 242 will ensure eventual quadratic convergence.

243 **The Newton operator.** Newton-type algorithms have been considered in the past, usually
 244 independently of other methods, and thus suffer from lack of global convergence. Moreover,
 245 from a numerical viewpoint, such methods face the *precision-control problem*. Our algorithm
 246 integrates subdivision with the Newton operator (an old idea that goes back to Dekker [17]
 247 in the 1960's), thus ensuring global convergence.

We want to find the Fermat point, i.e., the root of $\mathbf{f} = \nabla\varphi$. The Newton-type operators are well-studied in the interval literature, and they have the form $N = N_{\mathbf{f}} : \square\mathbb{R}^d \rightarrow \square\mathbb{R}^d$. There are three well-known versions of $N_{\mathbf{f}}$: the simplest version, from Moore [36] and Nickel [40], is

$$N(B) = m_B - J_{\mathbf{f}}^{-1}(B) \cdot \mathbf{f}(m_B),$$

where $J_{\mathbf{f}}$ is the Jacobian matrix of \mathbf{f} . Since $\mathbf{f} = \nabla\varphi$, this matrix is actually the Hessian of φ . The second version by Krawczyk [31, 52] is:

$$N(B) = m_B - K \cdot \mathbf{f}(m_B) + (I - K \cdot \mathbf{f}(B)) \cdot (B - m_B),$$

248 where K is any non-singular $d \times d$ matrix, usually chosen to be an approximation of $J_{\mathbf{f}}^{-1}(m_B)$.
 249 The third version, from Hansen and Sengupta [25, 24], can be viewed as a sophisticated
 250 implementation of the Moore-Nickel operator using an iteration reminiscent of the Gauss-
 251 Seidel algorithm, combined with preconditioning. Below we report on our implementation of
 252 the first two Newton operators. In general, the Newton operator $N(B)$ does not return a box
 253 even when B is a box; so we define $\square N(B)$ to be a box that contains $N(B)$. For simplicity,
 254 we assume that $\square N(B)$ is the smallest box containing $N(B)$ with the same aspect ratio as
 255 B .

256 The following properties of Newton box operators are consequences of Brouwer's Fixed
 257 Point Theorem [9, 41, 52, 59]:

- 258 1. (Inclusion Property) If $N(B) \subseteq B$ then $\mathbf{x}^* \in N(B)$.
 259 2. (Exclusion Property) If $N(B) \cap B = \emptyset$ then $\mathbf{x}^* \notin B$.
 260 3. (Narrowing Operator) If $\mathbf{x}^* \in B$ then $\mathbf{x}^* \in N(B)$.

261 Based on these properties, we can define two tests and an operator:

262 ► **Definition 6.** *Newton tests for gradient exclusion/inclusion predicates:*

- 263 ■ **Newton exclusion test:**
 264 $T_0^N(B) = \text{success}$ iff $N(2B) \cap B = \emptyset$. Thus $T_0^N(B) \Rightarrow C_0^\nabla(B)$.
 265 ■ **Newton inclusion test:**
 266 $T_1^N(B) = \text{success}$ iff $N(2B) \subseteq 2B$. Thus $T_1^N(B) \Rightarrow C_1^\nabla(2B)$. Below we explain
 267 why we use $2B$ instead of B .
 268 ■ **Newton narrowing operator:**
 269 $N_\cap(B)$ returns $B \cap N(2B)$.

270 Note that the Newton tests $T_0^N(B)$ and $T_1^N(B)$ are defined using the exact Newton
 271 operator $N(B)$. If we replace it by a soft version $\square N(B)$ in these definitions, they remain as
 272 inclusion/exclusion tests for $C_1^\nabla(B)/C_0^\nabla(B)$; we denote them by $\square C_1^\nabla(B)/\square C_0^\nabla(B)$.

273 To compute $\square N(B)$, we use standard interval arithmetic to evaluate the Moore & Nickel
 274 and Krawczyk operators. We already noted that if $N(B) \subseteq B$, then $\mathbf{x}^* \in N(B)$. But if \mathbf{x}^*
 275 is on the boundary of B , then $\square N(B) \subseteq B$ might not hold, and this issue persists even
 276 after splitting B . We circumvent this problem by using $2B$ instead of B in the definition of
 277 $T_1^N(B)$.

278 We enhance Algorithm 1 by the soft inclusion predicate $\square T_1^N(B)$, as sketched in Algo-
 279 rithm 2. If $\square T_1^N(B)$ succeeds, we conclude that \mathbf{x}^* is contained in $\square N(2B)$. In that case,
 280 we can discard all other boxes and initialize a new queue Q on $\square N(2B)$. In subsequent calls
 281 to $\square T_1^N(B')$ for $B' \in Q$, we conclude that $\mathbf{x}^* \in 2B'$. But to ensure that $w(2B') < w(B)$ (to
 282 avoid an infinite loop), we initialize the queue Q with the 4^d boxes of $\text{SPLIT}_2(\square N(2B))$.

■ **Algorithm 2** Enhanced subdivision for the approximate Fermat point (*ESUB*)

As in Algorithm 1 but replace line 5 with the following:

```

5.1 | if  $\square T_1^N(B)$  then
5.2 |   |  $Q \leftarrow \text{QUEUE}()$ ; // initialize a new queue
5.3 |   |  $Q.\text{PUSH}(\text{SPLIT}_2(\square N(2B)))$ ; // 2 SPLIT operations
5.4 | else
5.5 |   |  $Q.\text{PUSH}(\text{SPLIT}_1(B))$ ;

```

283 With respect to the runtime of Algorithm 2, we observe that once the soft Newton
 284 inclusion predicate succeeds, then it will also do so for an initial box of the new queue. This,
 285 essentially, divides the algorithm into two phases. The first phase can be basically seen as
 286 Algorithm 1. In the second phase, the Newton test guarantees quadratic convergence in ε .
 287 Getting into the second phase depends on the configuration of the foci set but not on ε ,
 288 hence, our approach is of particular interest for small values of ε .

289 The termination of both subdivision algorithms follows from the soft gradient exclusion
 290 predicate being convergent. The algorithms terminate once the predicate $C^\varepsilon(Q)$ succeeds,
 291 yielding an ε -approximate Fermat point, so we summarize as follows.

292 ► **Theorem 7.** *Both Algorithms 1 and 2 terminate and return an ε -approximate Fermat point.*

293 **3.3 Certifying the Weiszfeld method**

Weiszfeld’s iterative method [32, 43, 58] describes a sequence \mathbf{p}_i ($i = 0, 1, \dots$) of points that converges to the Fermat point \mathbf{x}^* , starting from any initial \mathbf{p}_0 . Each $\mathbf{p}_{i+1} = T(\mathbf{p}_i)$ where $T(\mathbf{x})$ is defined by

$$T(\mathbf{x}) = \frac{\sum_{\mathbf{a} \in A, \mathbf{a} \neq \mathbf{x}} w(\mathbf{a}) \frac{\mathbf{a}}{\|\mathbf{x} - \mathbf{a}\|}}{\sum_{\mathbf{a} \in A, \mathbf{a} \neq \mathbf{x}} w(\mathbf{a}) \frac{1}{\|\mathbf{x} - \mathbf{a}\|}}$$

294 Note that when \mathbf{x} is a focus, then $T(\mathbf{x})$ depends just on all other foci.

295 This simple iterative method is widely used, and although it converges, it does not solve
 296 our ε -approximation problem as we do not know when to stop. To see that this is a real
 297 issue, consider the example in Fig. 5.

298 We augment the Weiszfeld iteration by adding Newton tests during the computation,
 299 turning it into an ε -approximation algorithm. While at the i -th iteration, we define a small
 300 box B with point \mathbf{p}_i as center, and map it to the box $\square N(B)$ using the Newton operator;
 301 see Fig. 6. If $\square N(B) \subseteq B$, then the Fermat point \mathbf{x}^* lies in $\square N(B)$. On the contrary, if
 302 $\square N(B) \not\subseteq B$ we move on to the next point \mathbf{p}_{i+1} and adjust the box size as follows.

303 If $\frac{B}{10} \cap \square N(\frac{B}{10}) = \emptyset$, then the box $\frac{B}{10}$ does not contain \mathbf{x}^* and we therefore expand B by
 304 a factor of 10. If $\frac{B}{10} \cap \square N(\frac{B}{10}) \neq \emptyset$, then there might be a focus in box $\frac{B}{10}$, which hinders
 305 $\square N(B) \subseteq B$ to succeed. In that case we shrink B by a factor of 10. If a focus is not in $\frac{B}{10}$,
 306 shrinking B does not effect the algorithm negatively, as B can expand again.

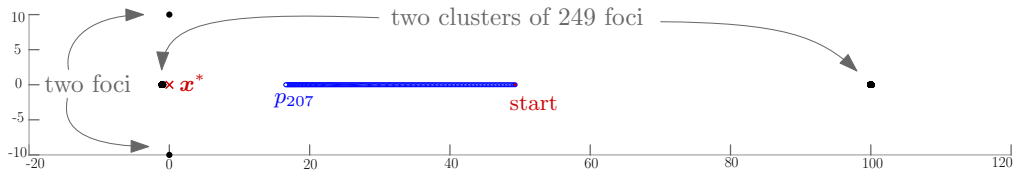
307 Using these tests we augment the point sequence scheme, sketched in Algorithm 3,
 308 with the property that if the Newton test evaluates to true, then we are guaranteed an
 309 ε -approximation of \mathbf{x}^* . As a starting point, we choose the *center of mass* \mathbf{p}_0 of A , i.e.,
 310 $\mathbf{p}_0 = \frac{1}{W} \sum_{\mathbf{a} \in A} w(\mathbf{a}) \mathbf{a}$.

■ **Algorithm 3** Certified Weiszfeld for the approximate Fermat point (*CW*)

Input: Foci set A , constant $\varepsilon > 0$	Output: Point $\tilde{\mathbf{x}}^*$
---	---

```

1  $\mathbf{p} \leftarrow \mathbf{p}_0; \quad l \leftarrow \varepsilon;$ 
2 while TRUE do
3    $B \leftarrow \text{Box } B(m_B = \mathbf{p}, \omega(B) = l);$ 
4   if  $\square N(B) \subseteq B$  then                                     // Fig. 6(a)
5      $\tilde{\mathbf{x}}^* \leftarrow \mathbf{p};$ 
6   else if  $\square N(\frac{B}{10}) \cap \frac{B}{10} = \emptyset$  then             // Fig. 6(b)
7      $l \leftarrow \min\{10 \cdot l, \varepsilon\};$ 
8   else                                                       // Fig. 6(c)
9      $l \leftarrow \frac{1}{10} \cdot l;$ 
10   $\mathbf{p} \leftarrow T(\mathbf{p});$ 
    
```



■ **Figure 5** An example with 500 foci, showing that Weiszfeld’s scheme does not solve the ε -approximation problem. The scheme stopped when $\|\mathbf{p}_{i-1} - \mathbf{p}_i\| \leq 1/10$, after 207 steps (blue points). The distance $\|\mathbf{x}^* - \mathbf{p}_{207}\|$ can be arbitrarily big ($\|\mathbf{x}^* - \mathbf{p}_{207}\| > 15$ in this case).

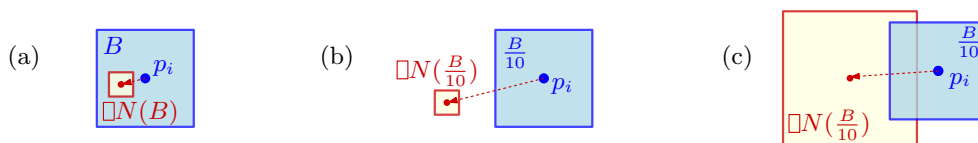


Figure 6 The three cases of Algorithm 3. (a) $N(B) \subseteq B$, (b) $N(B) \cap B = \emptyset$ and (c) $N(B) \cap B \neq \emptyset$.

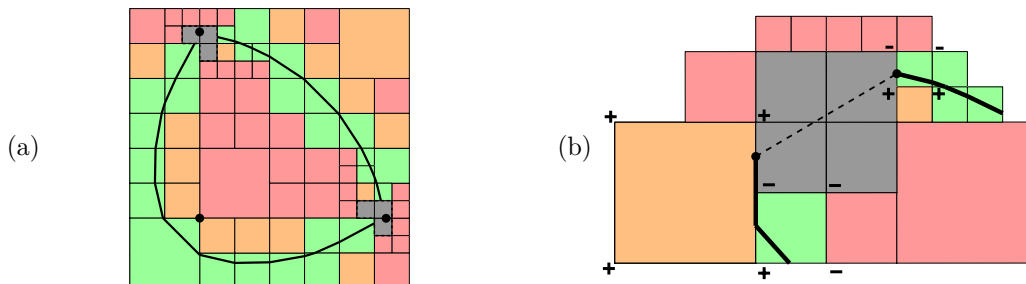


Figure 7 (a) A 3-ellipse passing through two foci. Components of gray boxes (temporarily) surround the foci. (b) If a gray component satisfies (B1) - (B3) the two ingoing edges are connected with an edge (shown dashed).

311 With respect to the runtime, the point sequence $T(\mathbf{x})$ converges linearly in ε towards
 312 \mathbf{x}^* [29] but in order for Algorithm 3 to terminate the test $\square N(B) \subseteq B$ must succeed. Similar
 313 to other Newton operators, $\square N(B) \subseteq B$ succeeds for boxes in a neighborhood surrounding
 314 \mathbf{x}^* . This neighborhood depends only on the configuration of A but not on ε . Further,
 315 evaluating $T(\mathbf{x})$ and $\square N(B)$ can be done in $O(nd^2)$ time. We conclude as follows.

316 ► **Theorem 8.** *Algorithm 3 terminates and returns an ε -approximate Fermat point.*

317 4 Approximating n -ellipses

318 In this section, we describe an algorithm to construct approximate n -ellipses, based on the
 319 subdivision paradigm. Throughout this work we maintain the subdivision *smooth*, i.e., the
 320 width of any two adjacent boxes, which are leaves of the quadtree, may differ at most by a
 321 factor of 2. Maintaining smoothness is easy to implement and has amortized $O(1)$ cost per
 322 operation [6]. Without maintaining smoothness, the amortized cost can be $\Omega(\log n)$ [6].

323 The Plantinga and Vegter (PV) construction [47, 33, 34] approximates the zero set of
 324 a function $F : \mathbb{R}^d \rightarrow \mathbb{R}$ where $d \in \{2, 3\}$. Assuming that $S = F^{-1}(0)$ is regular, i.e., the
 325 gradient ∇F is non-zero at every point of S , this approximation is isotopic to S . Our goal
 326 is to use this construction to approximate the n -ellipse defined by $F(p) := \varphi(p) - r$ with
 327 $r > r^*$. For simplicity, we assume all boxes are square; for the construction to succeed, we
 328 only need an aspect ratio $\leq \sqrt{2}$ (see [33]). We use the notation $\langle \cdot, \cdot \rangle$ for the scalar product.
 329 The following are the key predicates and tests in the PV construction of the n -ellipse $F^{-1}(0)$.

330 ► **Definition 9.** *Fix $F(p) = \varphi(p) - r$. Let B be a square box.*

- 331 1. *The fundamental box predicate is the inclusion predicate $C_1^F(B) : 0 \in F(B)$, and its*
 332 *complement, the exclusion predicate $C_0^F(B) : 0 \notin F(B)$.*
- 333 2. *The (corner) inclusion test $T_{cor}(B) = \text{success}$ iff F , when evaluated at the corners of B ,*
 334 *admits both negative and positive values. Clearly, $T_{cor}(B)$ is a test for $C_1^F(B)$. There is*
 335 *a standard PV trick whereby any 0-value can be arbitrarily made positive.*
- 336 3. *The normal variation predicate $C_{nv}(B)$ is defined by the condition $\langle \nabla F(B), \nabla F(B) \rangle > 0$.*

337 We obtain the soft versions $\square C_0^F(B)$ and $\square C_{nv}(B)$ by the usual device of replacing
 338 $F(B)$ in the definition of the predicates by a soft version $\square F(B)$. But for the inclusion
 339 predicate $C_1^F(B)$ we have no soft version. Instead, the corner test $T_{\text{cor}}(B)$ is a test for
 340 $C_1^F(B)$. To supplement the corner test, we need the normal variation predicate $C_{nv}(B)$. This
 341 predicate is equivalent to the condition that the angle between the gradient of any two points
 342 in B is at most 90° . It implies that the n -ellipse is monotone in either x - or y -direction
 343 within the box. In Fig. 7, boxes are: **red** if they pass the C_0^{Ex} test, **green** if they pass both
 344 $\square C_{nv}$ and T_{cor} , **orange** if they pass only $\square C_{nv}$, and **gray** otherwise. Note that orange boxes
 345 may, or may not, contain parts of the approximate n -ellipse.

346 An n -ellipse is not regular if it passes through some focus [51]; in that case a direct
 347 PV construction is not possible. To tackle this problem we develop a variation, where we
 348 simultaneously subdivide boxes and construct pieces of the n -ellipse *on the fly*, instead of
 349 doing that in the end. Further, boxes in which the n -ellipse may not be regular are treated
 350 differently. During the subdivision part of the algorithm, we classify boxes in three categories:

- 351 1. Boxes which satisfy C_0^{Ex} (**red**): These do not contain any piece of the n -ellipse, so they
 352 do not need to be further considered and are discarded.
- 353 2. Boxes which satisfy $\square C_{nv}$ and have width smaller than $\varepsilon/2$ (**green** or **orange**): We
 354 immediately draw edges in each of these boxes, in contrast to the normal PV construction.
 355 Note that at a later stage of the algorithm it might happen that we split one of B 's
 356 neighboring boxes. In that case we need to take into account the sign of F at the new
 357 vertex on B 's boundary. If necessary, the edges in box B then need to be updated.
- 358 3. The remaining boxes (**gray**): Such boxes occur near foci and need more careful attention,
 359 as we cannot apply the standard PV construction. Instead, given a set of gray boxes we
 360 first distinguish them in connected components, using a DFS algorithm. Then, for each
 361 connected component of gray boxes K_i , we check if a set of conditions is satisfied:

362 (B1) K_i contains exactly one focus.

363 (B2) There are exactly two PV-edges leading to K_i .

364 (B3) The distance between any two corners of the boxes in K_i is at most $\varepsilon/2$.

365 If K_i satisfies all (B1) - (B3), then we connect the 2 PV-edges leading to K_i by a line
 366 segment and discard boxes of K_i , see Fig. 7(b). Otherwise, the children of the boxes of
 367 K_i are put back in Q for further classification.

■ **Algorithm 4** Approximating an n -ellipse

Input: Foci set A , radius r , constant ε , box B_0	Output: Curve E
--	--------------------------

```

1  $Q \leftarrow \text{QUEUE}(); \quad Q.\text{PUSH}(B_0);$ 
2 while  $Q \neq \emptyset$  do
3    $Q_{\text{new}} \leftarrow \text{QUEUE}();$ 
4   while  $Q \neq \emptyset$  do
5      $B \leftarrow Q.\text{POP}();$ 
6     if not  $C_0^{\text{Ex}}(B)$  then
7       if  $\square C_{nv}(B)$  and  $\omega(B) < \varepsilon/2$  then
8          $E_{\cap B} \leftarrow \text{ONLINE-PV}(B);$ 
9       else
10         $Q_{\text{new}}.\text{PUSH}(\text{SPLIT}_4(B));$ 
11    $Q \leftarrow \text{CONNECTED-COMPONENTS-ANALYSIS}(Q_{\text{new}});$ 
12 return  $E;$ 

```

368 By controlling the size of the boxes containing parts of the output curve, and by the

369 modification the PV construction we prove the following.

370 ► **Theorem 10.** *Algorithm 4 returns an isotopic ε -approximation of the n -ellipse $F^{-1}(0)$.*

371 **Interpolating edges.** The PV construction creates edges within a box B , which start and
 372 end from midpoints of box edges. One can derive a nicer-looking approximation by using
 373 linear interpolation on the box edges by taking into account the value of F at B 's corners.

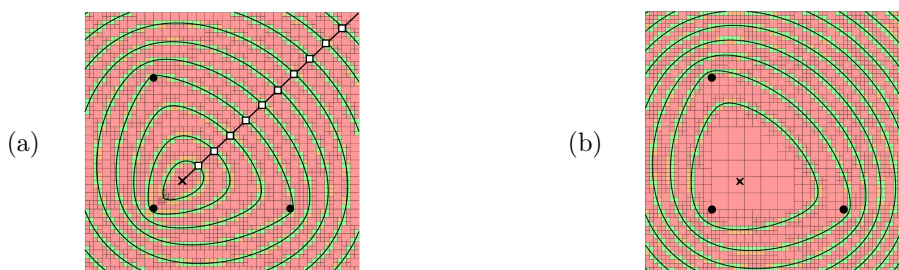
374 **Contour Plotting.** As an application, we can use the above technique in order to produce a
 375 topologically correct, ε -approximate and visually nice n -elliptic contour plot. To do so, we
 376 first adapt our algorithm in order to simultaneously plot several n -ellipses inside a bounding
 377 box, corresponding to the same foci but with different radii. Each n -ellipse is a *contour line*,
 378 and we describe how to plot them *visually nice*, i.e., the contour lines are roughly equally
 379 distributed in space. See Fig. 8 for two different approaches and their visualization effect.

380 5 Experiments

381 We implemented our algorithms for \mathbb{R}^2 and conducted a series of experiments. Our current
 382 software is written in Matlab (version R2018b), taking advantage of its graphics ability. The
 383 numerical accuracy is therefore IEEE numerical precision. The platform used was MacOS
 384 Big Sur v11.2.3, with 2.5 GHz Quad-Core Intel Core i7 and 16 GB 1600MHz DDR3.

385 Following, we report on our experiments, discussing some notable points one by one.
 386 We evaluated our algorithms on both synthetic and real-world datasets. For all algorithms
 387 approximating the Fermat point we chose a time limit of 600 seconds. Moreover, for most
 388 experiments we executed 10 different instances for completeness. In the illustrated charts,
 389 the curves pass through the mean of the 10 running times, and additionally we also marked
 390 the minimum and maximum running times. All axes in the charts are of logarithmic scale.

391 **Datasets.** We mainly experimented with two different types of synthetic datasets, namely
 392 UNIF-1 and UNIF-2. In UNIF-1 the n foci are sampled uniformly from a disk of radius 1. In
 393 UNIF-2 again the n foci are sampled uniformly from a disk of radius 1 and then $n/2$ foci are
 394 translated by a vector $(10, 10)$, see Fig. 9(a) and Fig. 9(b). Despite their similarity, the two
 395 datasets present strong differences. As we later see, UNIF-2 is significantly more difficult to
 396 solve in comparison to UNIF-1, and further UNIF-1 resembles nicely real-world datasets. The
 397 foci of UNIF-2 lie almost all on a common line, which implies that there are many points for
 398 which the gradient is close to 0. This makes it difficult to find the actual Fermat point, for
 399 which the gradient is exactly 0. We experimented with more types of synthetic datasets,



■ **Figure 8** Two different 3-elliptic contour plots with 10 contour lines, having the same set of foci.
 (a) Using radii of *equidistant points*. (b) Using *equidistant radii*.

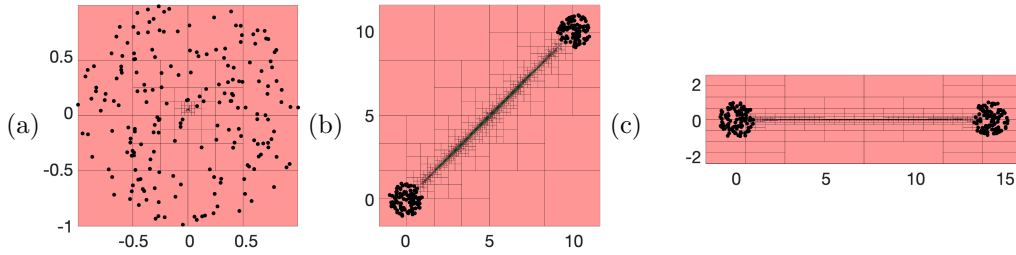


Figure 9 A box subdivision for $n = 200$ foci: (a) UNIF-1, (b) UNIF-2 and (c) UNIF-2 after PCA.

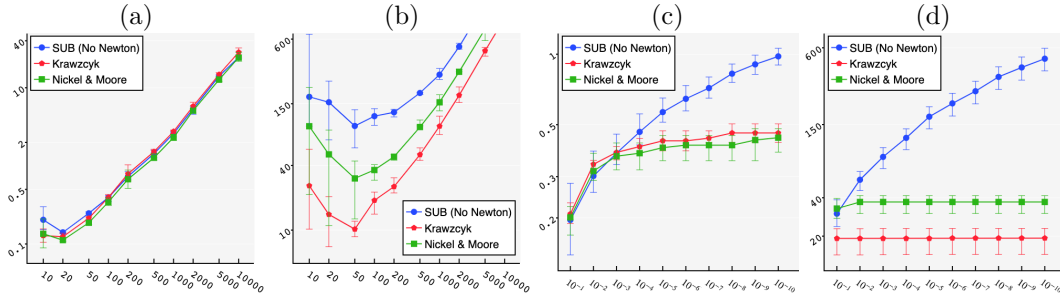


Figure 10 A comparison of Algorithm 1 (• SUB), Algorithm 2 with the Krawczyk Newton operator (• Krawczyk), and Algorithm 2 with the Nickel and Moore Newton operator (■ Nickel & Moore). (a),(b) Time as a function of n , with $\varepsilon = 10^{-4}$. (c),(d) Time as a function of ε with $n = 100$. (a),(c) UNIF-1 datasets. (b),(d) UNIF-2 datasets.

such as points in convex position, vertices of a regular n -gon, clusters of points, but we do not report on these results, as they are similar to UNIF-1 or UNIF-2.

Newton operators. Adding a Newton operator to the subdivision process drastically improves the running time. We compared Algorithm 1 with two versions of Algorithm 2, where we once use the Newton operator based on Moore and Nickel and also the operator by Krawczyk. The results for various values of n and ε on both UNIF-1 and UNIF-2 are summarized in Fig. 10. Note that Algorithm 2 initially needs to perform simple splitting operations until at some point the Newton test succeeds the first time. After that the algorithm converges quadratically in ε , which explains why the running time of both versions almost do not increase for decreasing ε . Even though the operator by Krawczyk returns a smaller box $\square N(B)$, i.e. it is more precise, than Moore and Nickel, it performs slower for UNIF-1 as evaluating the operator takes more time. We conclude that using a Newton operator speeds up the computations, and we use the one of by Moore and Nickel in Algorithm 2.

Principal component analysis. Foci sets like UNIF-2 are challenging as all foci are close to a common line. In this case, the subdivision algorithms can be slow because there are many boxes for which the gradient $\nabla\varphi$ is close to 0. Our approach to tackle this problem is to use subdivision with rectangular boxes. In a preprocessing step we do a *principal component analysis* (PCA) of the foci as heuristic. Then, we rotate the coordinate system such that the x -direction is the first principal component. In the box subdivision we use rectangular boxes with long x -width, see Fig. 9(c). Observe in the following table, that for well distributed foci sets like UNIF-1, using the PCA adds only a small overhead to the total running time.

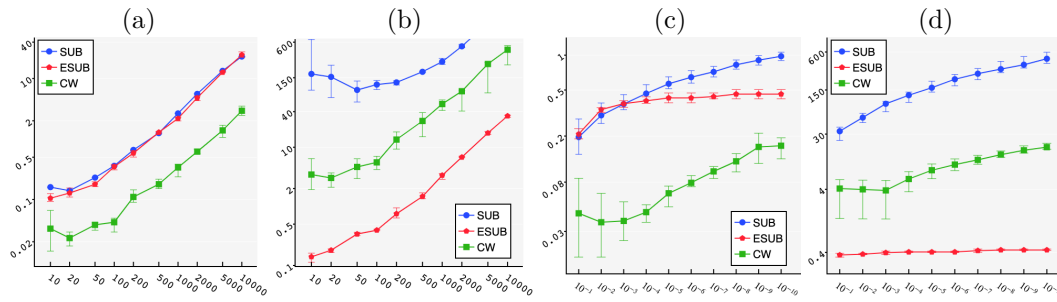


Figure 11 An overall comparison of Algorithm 1 (● SUB), Algorithm 2 with the PCA (◆ ESUB), and Algorithm 3 (■ CW). (a),(b) Time as a function of n , with $\varepsilon = 10^{-4}$. (c),(d) Time as a function of ε with $n = 100$. (a),(c) UNIF-1 datasets. (b),(d) UNIF-2 datasets.

$\varepsilon = 10^{-3}, n =$	10	100	1000	10000	$n = 100, \varepsilon =$	10^{-1}	10^{-3}	10^{-5}	10^{-7}
without PCA	0.12	0.31	2.33	23.4	without PCA	0.20	0.30	0.33	0.34
with PCA	0.10	0.30	2.30	23.9	with PCA	0.18	0.30	0.33	0.35

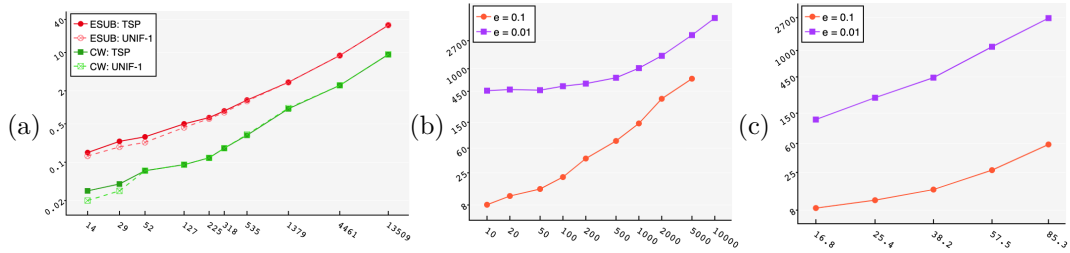
On the contrary, for sets like UNIF-2, adding the PCA decreases drastically the running time, as shown next. Hence, the PCA preprocessing is a useful addition to Algorithm 2, which we will use also in the following experiments.

$\varepsilon = 10^{-3}, n =$	10	100	1000	10000	$n = 100, \varepsilon =$	10^{-1}	10^{-3}	10^{-5}	10^{-7}
without PCA	90.7	48.5	170	timeout	without PCA	37.1	49.2	49.2	49.5
with PCA	0.15	0.40	3.21	32.7	with PCA	0.36	0.40	0.42	0.43

Real Datasets. Inspired by the applications in facility location we chose to experiment with instances of the well-known *Traveling Salesman Person Library* [49] or TSPLIB. The foci correspond mostly to location of cities in different areas around the world. It appears that real-world instances show a similar behavior to UNIF-1 datasets; so, UNIF-1 are realistic datasets for the evaluation of different algorithms. In our experiments illustrated in Fig. 12(a), for each TSPLIB dataset we created an additional foci set, where we uniformly sampled the same number of foci in the axis-aligned bounding box. As ε we chose 10^{-6} times the width of the corresponding bounding box. The similarity of the running time for the two datasets is obvious.

Summary on the Fermat point. We make an overall comparison of Algorithm 1, Algorithm 2 with the PCA, and Algorithm 3, illustrated in Fig. 11. The running time of all methods shows a linear dependency on n , but there are big differences regarding the dependency on ε . Overall, Algorithm 3 performs well in all cases, but due to the linear convergence of Weiszfeld’s point sequence, it cannot converge faster as ε decreases. In contrast, Algorithm 2 takes more time in the subdivision phase, but once the Newton tests succeeds, the algorithm terminates very quickly. So, it does not exhibit almost any changes in the running time for decreasing ε . This makes it favorable when a high precision approximate solution is required. It is also very fast in UNIF-2 instances and outperforms Algorithm 3. Summarizing, we suggest to use Algorithm 2 in small dimensional spaces and for small ε due to its eventual quadratic convergence in ε . On the other hand, the subdivision methods take exponential time in d , therefore, we suggest to use Algorithm 3 for higher dimensional spaces.

447 **n -ellipses.** Finally, we evaluated the runtime of n -ellipses algorithm. In Fig. 12(b) we
 448 evaluate the dependency on n . In order to keep the length of the curve almost constant
 449 we choose the radii $r = \frac{(10\sqrt{2}+2)n}{2}$. The bounding box used is $[-2, 12]^2$. In Fig. 12(c) we
 450 analyze the dependency on the length of the n -ellipse. The bounding box is fixed and we
 451 experimented with different radii such that the lengths of the curve differ by a factor of
 452 $3/2$. The runtime shows a linear dependency on n , as expected, and it also shows a linear
 453 dependency on the length of curve. This can be justified, as covering an n -ellipse of length l
 454 with boxes of width ε takes $O(l/\varepsilon)$ many boxes.



■ **Figure 12** (a) A comparison of TSP data sets (filled shapes) with UNIF-1(empty shapes, dashed curve) for both Algorithm 2 (● ESUB) and Algorithm 3 (■ CW). Fermat point with time as a function of n . (b)-(c) n -ellipse on UNIF-2 with time as a function of (b) n and (c) the length of the n -ellipse. Two ε approximations with $\varepsilon = 0.1$ (●) and $\varepsilon = 0.01$ (■) have been computed.

6 Concluding Remarks

455 In this work, we mainly focused on finding ε -approximate Fermat points, in a strong sense
 456 $\|\tilde{\mathbf{x}}^* - \mathbf{x}^*\| \leq \varepsilon$, which had not been considered before. This approximation can also be used to
 457 derive an ε -approximation of the Fermat radius. This was done using a simple-to-implement
 458 subdivision approach. All of our algorithms are certified in the sense of interval arithmetic.
 459 Moreover, we certified the famous point-sequence algorithm of Weiszfeld [58] to guarantee
 460 that it does find an ε -approximate Fermat point. We also designed an algorithm to construct
 461 ε -approximate n -ellipses. The simplicity and efficiency of our algorithms was evaluated
 462 experimentally.

464 There are many directions for further research. One is to derive algorithmic complexity
 465 bounds. Our intuition regarding the time complexity of our algorithms was affirmed by the
 466 experimental runtime evaluation. Such bounds are rare for iterative numerical algorithms.
 467 There has been considerable success in the area of root isolation [10, 11] where the idea of
 468 “continuous amortization” should also apply here. To improve our Newton operator, we plan
 469 to implement the Hansen-Sengupta [25, 24] version, and expect to see a speedup.

470 Regarding the construction of n -ellipses, it would be interesting to design an alternative
 471 algorithm based on curve-tracing. This could perform fast once a starting point on the
 472 n -ellipse is found.

473 Another direction is related to *Voronoi diagrams*. From one perspective, it is interesting
 474 to approximate the Voronoi diagram, where the sites are n -ellipses; so far only 2-ellipses have
 475 been studied [19]. From a different perspective, if the sites are sets of foci (each associated
 476 with a Fermat distance function) it is interesting to compute their Voronoi diagram, defined
 477 as the minimization diagram of the Fermat distance functions. This is a *min-sum* diagram
 478 in the context of cluster Voronoi diagrams, see e.g., [28, 44]. We believe that subdivision
 479 methods augmented with root boxes, similar to [5], would be applicable to these problems.

480 — **References** —

- 481 1 A. Karim Abu-Affash and Matthew J. Katz. Improved bounds on the average distance to
482 the Fermat-Weber center of a convex object. *Information Processing Letters*, 109(6):329–333,
483 2009.
- 484 2 Mihai Badoiu, Sariel Har-Peled, and Piotr Indyk. Approximate clustering via core-sets. In
485 *Proc. Symposium on Theory of Computing*, pages 250–257. ACM, 2002.
- 486 3 Chanderjit Bajaj. The algebraic degree of geometric optimization problems. *Discrete &
487 Computational Geometry*, 3(2):177–191, 1988.
- 488 4 Amir Beck and Shoham Sabach. Weiszfeld’s method: Old and new results. *Journal of
489 Optimization Theory and Applications*, 164(1):1–40, 2015.
- 490 5 Huck Bennett, Evanthia Papadopoulou, and Chee Yap. Planar minimization diagrams via
491 subdivision with applications to anisotropic Voronoi diagrams. *Computer Graphics Forum*,
492 35(5):229–247, 2016.
- 493 6 Huck Bennett and Chee Yap. Amortized analysis of smooth quadtrees in all dimensions.
494 *Computational Geometry*, 63:20–39, 2017.
- 495 7 Bhaswar B. Bhattacharya. On the Fermat-Weber point of a polygonal chain and its general-
496 izations. *Fundamenta Informaticae*, 107(4):331–343, 2011.
- 497 8 Prosenjit Bose, Anil Maheshwari, and Pat Morin. Fast approximations for sums of distances,
498 clustering and the Fermat-Weber problem. *Computational Geometry*, 24(3):135–146, 2003.
- 499 9 Luitzen Egbertus Jan Brouwer. Über Abbildung von Mannigfaltigkeiten. *Mathematische
500 Annalen*, 71(1):97–115, 1911.
- 501 10 Michael Burr, Felix Kraemer, and Chee Yap. Continuous amortization: A non-probabilistic
502 adaptive analysis technique. *Electronic Colloquium on Computational Complexity*, TR09(136),
503 2009.
- 504 11 Michael A. Burr. Continuous amortization and extensions: With applications to bisection-based
505 root isolation. *Journal of Symbolic Computation*, 77:78–126, 2016.
- 506 12 Paz Carmi, Sariel Har-Peled, and Matthew J. Katz. On the Fermat-Weber center of a convex
507 object. *Computational Geometry*, 32(3):188–195, 2005.
- 508 13 Hui Han Chin, Aleksander Madry, Gary L. Miller, and Richard Peng. Runtime guarantees for
509 regression problems. In *Proc. Innovations in Theoretical Computer Science*, pages 269–282.
510 ACM, 2013.
- 511 14 Dietmar Cieslik. *Steiner minimal trees*, volume 23. Springer Science & Business Media, 2013.
- 512 15 Ernest J. Cockayne and Zdzislaw A. Melzak. Euclidean constructibility in graph-minimization
513 problems. *Mathematics Magazine*, 42(4):206–208, 1969.
- 514 16 Michael B. Cohen, Yin Tat Lee, Gary L. Miller, Jakub Pachocki, and Aaron Sidford. Geometric
515 median in nearly linear time. In *Proc. Symposium on Theory of Computing*, pages 9–21. ACM,
516 2016.
- 517 17 Theodorus Jozef Dekker. Finding a zero by means of successive linear interpolation. In
518 *Constructive Aspects of the Fundamental Theorem of Algebra*, pages 37–48. Wiley Interscience,
519 1967.
- 520 18 Adrian Dumitrescu, Minghui Jiang, and Csaba D. Tóth. New bounds on the average distance
521 from the Fermat-Weber center of a planar convex body. *Discrete Optimization*, 8(3):417–427,
522 2011.
- 523 19 Ioannis Z. Emiris, Elias P. Tsigaridas, and George M. Tzoumas. The predicates for the Voronoi
524 diagram of ellipses. In *Proc. Symposium on Computational Geometry*, pages 227–236. ACM,
525 2006.
- 526 20 Giovanni Francesco Fagnano. Problemata quaedam ad methodum maximorum et minimorum
527 spectantia. *Nova Acta Eruditorum*, pages 281–303, 1775.
- 528 21 Sándor P Fekete, Joseph SB Mitchell, and Karin Beurer. On the continuous Fermat-Weber
529 problem. *Operations Research*, 53(1):61–76, 2005.
- 530 22 Dan Feldman and Michael Langberg. A unified framework for approximating and clustering
531 data. In *Proc. Symposium on Theory of Computing*, pages 569–578. ACM, 2011.

- 532 23 Horst Hamacher and Zvi Drezner. Facility location: applications and theory. *Science &*
533 *Business Media: Springer*, 2002.
- 534 24 Eldon R. Hansen. A multidimensional interval newton method. *Reliable Computing*, 12(4):253–
535 272, 2006. doi:10.1007/s11155-006-9000-y.
- 536 25 Eldon R. Hansen and Saumyendra Sengupta. Bounding solutions of systems of equations
537 using interval analysis. *BIT*, 21:203–211, 1981.
- 538 26 Sarel Har-Peled and Akash Kushal. Smaller coresets for k-median and k-means clustering.
539 *Discrete & Computational Geometry*, 37(1):3–19, 2007.
- 540 27 Sarel Har-Peled and Soham Mazumdar. On coresets for k-means and k-median clustering. In
541 *Proc. 36th Annual ACM Symposium on Theory of computing*, pages 291–300. ACM, 2004.
- 542 28 Daniel P Huttenlocher, Klara Kedem, and Micha Sharir. The upper envelope of Voronoi
543 surfaces and its applications. *Discrete & Computational Geometry*, 9(3):267–291, 1993.
- 544 29 I. Norman Katz. Local convergence in Fermat’s problem. *Mathematical Programming*, 6(1):89–
545 104, 1974.
- 546 30 Jakob Krarup and Steven Vajda. On Torricelli’s geometrical solution to a problem of Fermat.
547 *Journal of Management Mathematics*, 8(3):215–224, 1997.
- 548 31 Rudolf Krawczyk. Newton-Algorithmen zur Bestimmung von Nullstellen mit Fehlerschranken.
549 *Computing*, 4(3):187–201, 1969.
- 550 32 Harold W. Kuhn. A note on Fermat’s problem. *Mathematical programming*, 4(1):98–107, 1973.
- 551 33 Long Lin and Chee Yap. Adaptive isotopic approximation of nonsingular curves: the parame-
552 terizability and nonlocal isotopy approach. *Discrete & Computational Geometry*, 45(4):760–795,
553 2011.
- 554 34 Long Lin, Chee Yap, and Jihun Yu. Non-local isotopic approximation of nonsingular surfaces.
555 *Computer-Aided Design*, 45(2):451–462, 2012.
- 556 35 Luis Fernando Mello and Lucas Ruiz dos Santos. On the location of the minimum point in the
557 Euclidean distance sum problem. *São Paulo Journal of Mathematical Sciences*, 12:108–120,
558 2018.
- 559 36 Ramon E Moore. *Interval Analysis*, volume 4. Prentice-Hall Englewood Cliffs, NJ, 1966.
- 560 37 Kent E Morrison. The fedex problem. *The College Mathematics Journal*, 41(3):222–232, 2010.
- 561 38 Gyula Sz Nagy. Tschirnhaus’sche Eiflächen und Eikurven. *Acta Mathematica Academiae*
562 *Scientiarum Hungarica*, 1(1):36–45, 1950.
- 563 39 Nguyen Mau Nam. The Fermat-Torricelli problem in the light of convex analysis. *ArXiv*
564 *e-prints*, November 2013. arXiv:1302.5244v3.
- 565 40 Karl Nickel. Triplex-algol and applications. *Interner Bericht des Instituts für Informatik der*
566 *Universität Karlsruhe*, 1969.
- 567 41 Karl Nickel. On the Newton method in interval analysis. Technical report, Wisconsin
568 University-Madison Mathematics Research Center, 1971.
- 569 42 Jiawang Nie, Pablo A. Parrilo, and Bernd Sturmfels. Semidefinite representation of the
570 k-ellipse. In *Algorithms in algebraic geometry*, pages 117–132. Springer, 2008.
- 571 43 Lawrence M Ostresh Jr. Convergence and descent in the Fermat location problem. *Trans-*
572 *portation Science*, 12(2):153–164, 1978.
- 573 44 Evanthia Papadopoulou. The Hausdorff Voronoi diagram of point clusters in the plane.
574 *Algorithmica*, 40(2):63–82, 2004.
- 575 45 Pablo A. Parrilo and Bernd Sturmfels. Minimizing polynomial functions. *Algorithmic and*
576 *quantitative real algebraic geometry, DIMACS Series in Discrete Mathematics and Theoretical*
577 *Computer Science*, 60:83–99, 2003.
- 578 46 Maja Petrović, Bojan Banjac, and Branko Malešević. The geometry of trifocal curves with
579 applications in architecture, urban and spatial planning. *Spatium*, pages 28–33, 2014.
- 580 47 Simon Plantinga and Gert Vegter. Isotopic approximation of implicit curves and surfaces.
581 In *Proc. of the Eurographics/ACM SIGGRAPH Symposium on Geometry Processing*, pages
582 245–254. ACM, 2004.

- 583 **48** Helmut Ratschek and Jon Rokne. *Computer methods for the range of functions*. Horwood,
584 1984.
- 585 **49** Gerhard Reinelt. TSPLIB - A traveling salesman problem library. *ORSA Journal on Computing*,
586 3(4):376–384, 1991.
- 587 **50** Hanan Samet. *The Design and Analysis of Spatial Data Structures*. Addison-Wesley, 1990.
- 588 **51** Junpei Sekino. n-ellipses and the minimum distance sum problem. *The American mathematical*
589 *monthly*, 106(3):193–202, 1999.
- 590 **52** Sergey P Shary. Krawczyk operator revised. *Novosibirsk, Institute of Computational Tech-*
591 *nologies, Rússia*, 2004.
- 592 **53** Rudolf Sturm. Über den Punkt kleinster Entfernungssumme von gegebenen Punkten. *Journal*
593 *für die reine und angewandte Mathematik*, 97:49–61, 1884.
- 594 **54** Warwick Tucker. *Validated Numerics: A short intro to rigorous computations*. Princeton
595 Press, 2011.
- 596 **55** Ehrenfried Walther von Tschirnhaus. *Medicina Mentis Et Corporis*. Fritsch, Lipsiae, 1695.
597 URL: <http://mdz-nbn-resolving.de/urn:nbn:de:bvb:12-bsb10008248-3>.
- 598 **56** Cong Wang, Yi-Jen Chiang, and Chee Yap. On soft predicates in subdivision motion planning.
599 *Computational Geometry: Theory and Applications.*, 48(8):589–605, September 2015.
- 600 **57** Alfred Weber. Über den Standort der Industrien. *English translation by CJ Friedrich (1929)*
601 *Theory of the Location of Industries*, 1909.
- 602 **58** Endre Weiszfeld. Sur le point pour lequel la somme des distances de n points donnés est
603 minimum. *Tohoku Mathematical Journal, First Series*, 43:355–386, 1937.
- 604 **59** Juan Xu and Chee Yap. Effective subdivision algorithm for isolating zeros of real systems
605 of equations, with complexity analysis. In *Proc. International Symposium on Symbolic and*
606 *Algebraic Computation*, pages 399–406. ACM, 2019.
- 607 **60** Guoliang Xue and Yinyu Ye. An efficient algorithm for minimizing a sum of Euclidean norms
608 with applications. *SIAM Journal on Optimization*, 7(4):1017–1036, 1997.